

# PCCP

Accepted Manuscript



This is an Accepted Manuscript, which has been through the Royal Society of Chemistry peer review process and has been accepted for publication.

Accepted Manuscripts are published online shortly after acceptance, before technical editing, formatting and proof reading. Using this free service, authors can make their results available to the community, in citable form, before we publish the edited article. We will replace this Accepted Manuscript with the edited and formatted Advance Article as soon as it is available.

You can find more information about Accepted Manuscripts in the [author guidelines](#).

Please note that technical editing may introduce minor changes to the text and/or graphics, which may alter content. The journal's standard [Terms & Conditions](#) and the ethical guidelines, outlined in our [author and reviewer resource centre](#), still apply. In no event shall the Royal Society of Chemistry be held responsible for any errors or omissions in this Accepted Manuscript or any consequences arising from the use of any information it contains.



Journal Name

PERSPECTIVE

## Electrochemical hydrogenation of non-aromatic carboxylic acid derivatives as a sustainable synthesis process: from catalyst design to device construction

Received 00th January 20xx,  
Accepted 00th January 20xx

Masaaki Sadakiyo,<sup>a,b</sup> Shinichi Hata,<sup>c</sup> Takashi Fukushima,<sup>a</sup> Gergely Juhász,<sup>d\*</sup> Miho Yamauchi<sup>a,b\*</sup>

DOI: 10.1039/x0xx00000x

www.rsc.org/

**Electrochemical hydrogenation of a carboxylic acid using water as a hydrogen source is an environmentally friendly synthetic process for upgrading bio-based chemicals. We systematically studied electrochemical hydrogenation of non-aromatic carboxylic acid derivatives on anatase TiO<sub>2</sub> by combination of experimental analyses and density functional theory calculations, which first shed light on mechanistic insights for the electrochemical hydrogenation of carboxylic acids. Development of a substrate permeable TiO<sub>2</sub> cathode enabled construction of a flow-type electrolyser, i.e., a so-called polymer electrode alcohol synthesis cell (PEAEC) for the continuous synthesis of an alcoholic compound from a carboxylic acid. We demonstrated the highly efficient and selective conversion of oxalic acid to produce glycolic acid, which can be regarded a direct electric power storage into easily treatable alcoholic compound.**

### 1. Introduction

Material synthesis using electric power produced from renewable energies, i.e., renewable electricity, would accelerate the realisation of sustainable society where CO<sub>2</sub> emission is minimised by suppressing consumption of fossil fuels. Especially, electro-synthesis using water as a hydrogen source makes it possible to synthesise fully environmentally friendly compounds, although thermal hydrogenation is a main stream in the present industrial process as long as cheap hydrogen derived from fossil resources is available. Recently, progress in electro-synthesis using CO<sub>2</sub> as a carbon source showed striking progress, which enables selective production of raw materials, such as CO,<sup>1</sup> HCOOH,<sup>2,3</sup> ethanol,<sup>4,5,6</sup> ethylene<sup>7</sup>

and so on. Note that it is a major challenge to recycle dilute CO<sub>2</sub> from air, and to find cost-effective ways to separate and concentrate CO<sub>2</sub>.<sup>8</sup> Bio-derived carbon materials converted from atmospheric CO<sub>2</sub> are regarded as a body of concentrated CO<sub>2</sub> and therefore should be more actively utilised as a carbon source. A representative chemical converted from biomass is bio-alcohol, that is produced via fermentation of glucose and already becomes commercially available.<sup>9</sup> However, utilisation of glucose competes demand as foodstuffs and stoichiometric yield for ethanol production is 51%, which limits efficiency. Organic acids are abundantly contained in biomass and seem to be a useful carbon resource for the production of chemicals.<sup>10</sup> Recently, alcohol production via hydrogenation of an organic acid draws attentions for the purpose of upgrading bio-based feedstocks.<sup>11,12</sup>

A carboxylic group included in organic acids is chemically stable due to low electrophilicity of carbonyl carbon placed on

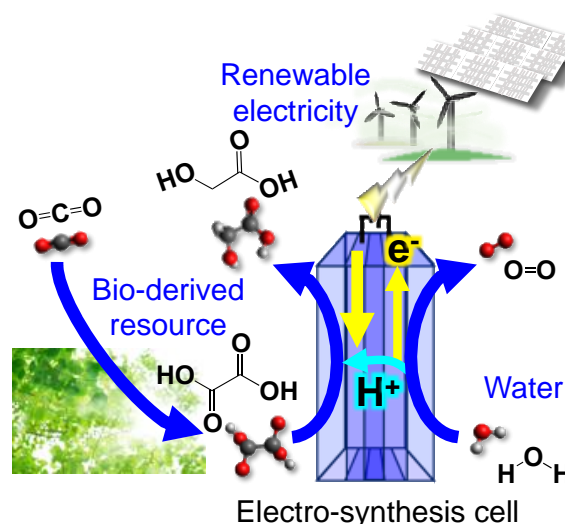


**Figure 1.** Schematic image of environmentally friendly hydrogenation of a bio-derived carboxylic acid using water and electricity produced from renewable energies.

<sup>a</sup> International Institute for Carbon-Neutral Energy Research (WPI-I2CNER), Kyushu University, Moto-oka 744, Nishi-ku Fukuoka 819-0395, Japan.

<sup>b</sup> Department of Chemistry, Faculty of Science, Kyushu University, Moto-oka 744, Nishi-ku Fukuoka 819-0395, Japan

<sup>c</sup> Department of Applied Chemistry, Tokyo University of Science Yamaguchi, Sanyo-Onoda, Yamaguchi 756-0884.

<sup>d</sup> Department of Chemistry, Graduate School of Science, Tokyo Institute of Technology, Ookayama, Meguro-ku, Tokyo, 152-8550, Japan.

† Electronic Supplementary Information (ESI) available: See DOI: 10.1039/x0xx00000x

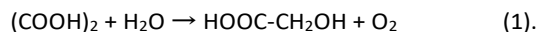
a conjugation system formed on an O-C-O bond, therefore the hydrogenation of carboxylic acids is hard to achieve.<sup>13</sup> Generally, progress of the hydrogenation of a carboxylic acid needs application of high-pressure H<sub>2</sub> at high temperatures or highly active hydrides made from fossil originated hydrogen, which impairs the significance of utilisation of a bio-derived carbon source. We, then, focus on electro-reduction using water as a hydrogen source (Figure 1).

The electro-reduction of some aromatic carboxylic acids, such as anthranilic acid<sup>13</sup> and isophthalic acid, has been reported, whereas the reduction of non-aromatic carboxylic acids is much more difficult. One of difficulties for the onset of electro-reduction of non-aromatic carboxylic acids, that they are mainly soluble in water, where the hydrogen evolution competes with the electro-reduction of carboxylic acids. Metallic catalysts, such as Pt nanoparticles are known to exhibit low overpotential for hydrogen evolution, and therefore, electro-reduction of carboxylic acids on metal catalysts hardly occurs due to preferential progress of hydrogen production. So far, some researchers realized electro-reduction of oxalic acid, a divalent carboxylic acid, using TiO<sub>2</sub> electrode<sup>15</sup> whereas the reduction is only achievable on metallic electrode with high overpotential for hydrogen evolution,<sup>16, 17</sup> e.g., Pb, Tl and Hg. The main product in the electro-reduction of oxalic acid has been glyoxylic acid, 2-electron reduction compound. Recently, we succeeded in highly selective production of glycolic acid, a monovalent alcoholic compound, via electro-reduction of oxalic acid by using pure anatase TiO<sub>2</sub> electrode.<sup>18,19,20</sup> Noted that glycolic acid is applicable to skincare cosmetics, preservatives, perfumes, biodegradable polymers and so on. This electro-reduction is meaningful in terms not only of the electro-synthesis of an alcoholic compound from a carboxylic acid but also of direct electric power storage in a water-soluble chemical, i.e., easy-to-handle liquid carrier. Furthermore, we also achieved direct light-energy storage into glycolic acid though oxalic acid reduction<sup>21</sup> and the first construction of an electrolyser that can continuously produce glycolic acid from oxalic acid and water.<sup>22</sup> However, glycolic acid production from oxalic acid is still a rare example of alcohol production from non-aromatic carboxylic acid. Thus, in this perspective, we show the other examples of electro-reduction of carboxylic acids as well as elucidated the reaction mechanism, which first uncovers fundamental principles of electro-reduction of carboxylic acid derivatives through experimental and theoretical approaches. We also introduce a high-performance electrolyser for the production of an alcoholic compound from a carboxylic acid, which will be available not only for the alcohol production but also for electric power storage.

## 2. Electro-reduction of oxalic acid on anatase TiO<sub>2</sub>

Alcohol production via thermal hydrogenation of carboxylic acids in organic processes has been intensively studied whereas the limited number of researches concerning electro-reduction of carboxylic acid in an aqueous phase have been achieved as mentioned above. Oxalic acid was selectively reduced into glycolic acid on TiO<sub>2</sub> electrode in an aqueous media. The reaction involves 4-electron reduction using electrons

generated via water oxidation at anode as described in the following equation:



Notably, the structure of TiO<sub>2</sub> is a crucial factor for the acceleration of the reaction. Anatase TiO<sub>2</sub> electrode can efficiently converts oxalic acid into glycolic acid, whereas only small amount of oxalic acid is reduced on rutile TiO<sub>2</sub>.<sup>18</sup> Based on the fact that anatase and rutile TiO<sub>2</sub> phases show characteristic energy energy-loss spectral (EELS) patterns,<sup>18</sup> we examined phase distribution on active and inactive TiO<sub>2</sub> catalysts by the spectral shape recognition of each phase using a scanning transmission electron microscopy (STEM) instrument equipped with an EELS analyser and produce an EELS map for the two phases, as shown in Figures 2a-2d. The EELS map revealed that an active catalyst is composed of purely anatase TiO<sub>2</sub>, and an inactive one includes a layer rutile TiO<sub>2</sub> around the surface (Figures 2e and 2f). We suggested that energy level of the conduction-band-bottom (CBB) of TiO<sub>2</sub> is significantly important for the 4-electron reduction of oxalic acid to glycolic acid. Electrons introduced into CBB of anatase can overcome overpotential for oxalic acid reduction whereas the reaction is hardly initiated on rutile TiO<sub>2</sub> with lower energy level of CBB (Figure 2g).

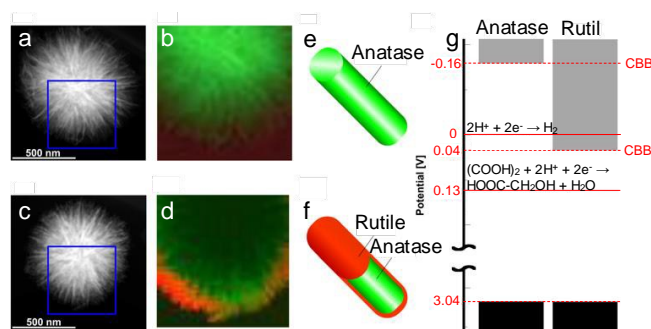


**Figure 2.** EELS maps of anatase and rutile phases on TiO<sub>2</sub> and energy diagrams of anatase- and rutile-type TiO<sub>2</sub>. (a) and (c) STEM images of active and inactive TiO<sub>2</sub> catalysts. (b) and (d) EELS maps of Ti L3-edge signals in the area marked by red squares in (a) and (c). The EELS signal intensities from the anatase and rutile phases are recognized by green and red colours, respectively. Illustrations for distributions of anatase and rutile phases in (e) active and inactive TiO<sub>2</sub>. (g) Energy diagrams of conduction and valence bands for anatase- and rutile-type TiO<sub>2</sub> conduction and valence bands and redox potentials for H<sub>2</sub> and glycolic acid evolutions. Adapted from Ref. 18 with permission from The Royal Society of Chemistry.

## 3. Reactivity of carboxylic acid derivatives on anatase TiO<sub>2</sub>

Oxalic acid is classified as an  $\alpha$ -keto acid having a carbonyl group at  $\alpha$  position of the carboxylic acid. We already elucidated that oxalic acid reduction proceeds through successive 2-electron reductions,<sup>17</sup> which implies that 4 electrons are hardly introduced into a carbonyl group at a time. We assumed that carbonyl group connected at  $\alpha$ -position

perhaps lowers energy of a transition state through extension of electron distribution over a conjugation system. Based on this assumption, an electron withdrawing group may play a similar role of a carboxy group to stabilise the excitation state. Molecular structure, that considerably affects the energy of the transition state, might be also relevant to the reactivity. Then, we examined reducibility of carboxylic acid having at a different functional group at  $\alpha$ -position.

We selected 11 carboxylic acids (R-COOH) as a substrate based on the different delocalization and electron withdrawing effect of their side chains: saturated fatty acid ( $-R = -H$  (formic acid),  $-CH_3$  (acetic acid)),  $\alpha$ -keto acid ( $-R = -CONH_2$  (oxamic acid),  $-CHO$  (glyoxylic acid),  $-COCH_3$  (pyruvic acid),  $-COC_3H_7$  (2-oxopentanoic acid),  $-CO(CH_2)_2COOH$  ( $\alpha$ -ketoglutaric acid),  $-COC(CH_3)_3$  (trimethylpyruvic acid)), and unsaturated fatty acid ( $-R = -CHCH_2$  (acrylic acid),  $-CHCHCOOH$  (fumaric acid), and  $-CH_2OH$  (glycolic acid)). All substrates are summarized in Table 1. We conducted electrochemical hydrogenation of carboxylic acid derivatives on the anatase TiO<sub>2</sub> electrode.

**Table 1.** Classification of the substrates by molecular features, conversion of carboxylic acid and Faradaic efficiency for an alcoholic compound on the cathode side after chronoamperometry ( $-0.7$  V (vs. RHE) at  $50$  °C (except for 2-oxopentanoic acid and  $\alpha$ -ketoglutaric acid) for 2 h).

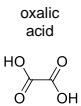
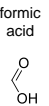
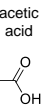
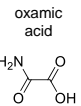
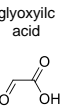
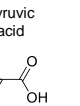
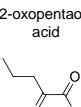
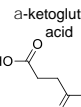
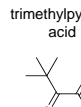
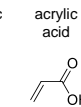
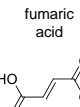
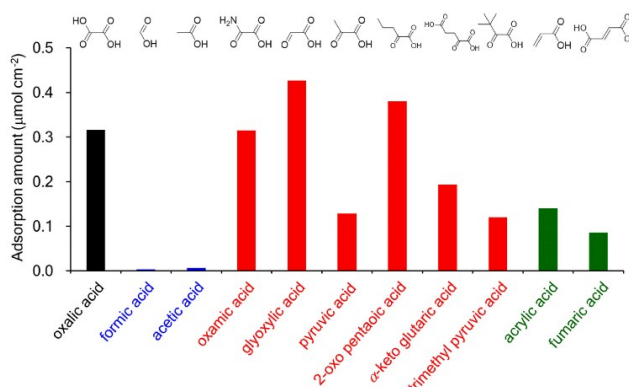
						
classification of substrate	$\alpha$ -keto acid (divalent)	sat. fatty acid	sat. fatty acid	$\alpha$ -keto acid	$\alpha$ -keto acid	$\alpha$ -keto acid
conv. (%)	29	0	0	12	96	65
FE (%)	58	0	0	0.2	88	90
						
classification of substrate	$\alpha$ -keto acid	$\alpha$ -keto acid (divalent)	$\alpha$ -keto acid	unsat. fatty acid	unsat. fatty acid (divalent)	
conv. (%)	60 (※at 25 °C)	92 (※at 25 °C)	57	6	100	
FE (%)		-	99	8.7	86	

Table 1 shows a summary of the conversion of the substrate and Faradaic efficiency for the production of corresponding alcoholic compound in the electro-reduction at  $-0.7$  V (vs. RHE) for 2 h. Formic acid and acetic acid were not converted into the reduced product such as aldehyde and alcohol, indicating that the saturated fatty acid is not reactive in our experimental condition. On the other hand, almost all of  $\alpha$ -keto acid (glyoxylic acid, pyruvic acid, 2-oxopentanoic acid,  $\alpha$ -ketoglutaric acid, and trimethylpyruvic acid) showed high conversion of the substrate in range from 53% to 95% except for oxamic acid (12%). Characterization of the products through the HPLC clearly confirmed that the reduced product of the  $\alpha$ -keto acids is an  $\alpha$ -hydroxy acid, indicating that the hydrogenation of carboxylic

acid group hardly occur whereas the carbonyl group on the  $\alpha$  position was electrochemically reduceable. This result is probably related to the fact that oxalic acid (divalent carboxylic acid) do not give ethylene glycol (divalent alcohol) but glycolic acid ( $\alpha$ -hydroxy acid), in our previous report.<sup>18</sup> In the case of unsaturated fatty acids, fumaric acid was almost completely converted whereas slight amount of acrylic acid was converted (6%). The product from fumaric acid was a saturated carboxylic acid, i.e., succinic acid, implying that the hydrogenation of the C=C double bond neighboring to the carboxylic acid group proceeds. These results indicate that the hydrogenation of carboxylic acid derivatives preferentially occurs on the unsaturated functional group (C=O and C=C) adjacent to the carboxylic acid group rather than the carboxylic acid group.



**Figure 3.** Amount of various substrates adsorbed on the cathode electrode ( $2 \times 2$  cm<sup>2</sup>, TiO<sub>2</sub>-coated Ti). Blue, red, and green color indicates saturated fatty acid,  $\alpha$ -keto acid, and unsaturated fatty acid, respectively.

Considering the reactivity and similarity in molecular structure between the acrylic acid (not reactive) and fumaric acid (or between oxamic acid (not reactive) and other  $\alpha$ -keto acids), the reactivity of the carboxylic acid derivatives for the electrochemical hydrogenation reaction does not simply depend on the molecular structure, but on other factors.

For the hydrogenation of a substrate molecule, electrons and protons are transferred from the electrode and the aqueous solution, respectively. This requires a strong interaction between the electrode and substrate as it was already pointed out in the literature.<sup>23</sup> Thus, we assume three key steps for the progress of hydrogenation of carboxylic acid derivatives on a TiO<sub>2</sub> catalyst: (i) adsorption of a substrate molecule through making a bond between carboxylic acid group and TiO<sub>2</sub> surface, (ii) protonation and electron injection from electrode to a substrate and (iii) elimination of a product from the catalyst. Some of dominant factors for making significant difference in the reactivity among the carboxylic acid derivatives probably exist in these reaction steps.

#### 4. Relationship between adsorption ability of carboxylic acid derivatives on anatase TiO<sub>2</sub> and reactivity

To clarify adsorption ability of the carboxylic acid derivatives on the TiO<sub>2</sub> surface was tested by immersion of the catalytic electrode (TiO<sub>2</sub>-decorated Ti) into the substrate solution for 2 h

at room temperature. Figure 3 shows the amount of carboxylic acid derivatives adsorbed on anatase TiO<sub>2</sub>. In the case of saturated fatty acids, both of formic acid and acetic acid did not show remarkable adsorption of the substrate (less than 0.006  $\mu\text{mol cm}^{-2}$ ), which seems to be consistent with no reactivity of these substrate. In contrast, all of  $\alpha$ -keto acids and unsaturated fatty acids showed a large amount of adsorption in range from 0.086 to 0.427  $\mu\text{mol cm}^{-2}$ , which is consistent with the previous reports suggesting the strong affinity of carboxylic acids for the TiO<sub>2</sub> surface. Considering the fact that the oxamic acid and acrylic acid is not highly reactive for the electrochemical hydrogenation on the TiO<sub>2</sub>, there should be another dominant factor for controlling the reactivity of the carboxylic acid derivatives. Seeing the molecular structures of the substrates, the difference in the adsorption property among them is possibly attributed to the existence of unsaturated group neighboring to the carboxylic acid, which should cause differences in the adsorption through various factors such as adsorption configuration or electronic interaction with TiO<sub>2</sub>.

### 5. Relationship between energy levels of LUMO of the substrates and reactivity

Density functional theory calculations were performed to understand the trend of the reduction reaction of the carboxylic acid molecules and the reaction mechanism. We estimated the energy levels of the lowest unoccupied molecular orbitals (LUMO) of the substrates, which should directly relate with acceptability of electrons from the electrode (or stability of the reduced species) in the hypothesized second step (i.e. electron injection). Figure 4 shows energy levels of LUMO (and HOMO) and orbitals of the LUMO of the substrates. The energy level of the LUMO of formic acid and acetic acid is calculated to be 0.002 and 0.255 eV, respectively. These values are remarkably high compared to other substrates,  $\alpha$ -keto acids and unsaturated carboxylic acids ( $< -1.345$  eV), due to the conjugation between the unsaturated group (e.g. C=O and C=C) and the carboxylic acid group. All of the substrates with unsaturated group neighboring to the carboxylic acid group showed relatively low LUMO levels in range from  $-2.625$  to  $-1.487$  eV. Note that, in these molecules, the LUMO levels of oxamic acid ( $-1.487$  eV) and acrylic acid ( $-1.345$  eV) showed slightly higher LUMO level compared to those of the other derivatives (from  $-2.503$  to  $-1.968$  eV). The schematic view of the of LUMO is shown in the Figure 4. All of the LUMO in the carboxylic acids is composed of 2p atomic orbitals of O1, C1, and O2 on the  $-\text{COOH}$  with opposite phases against the orbitals on the neighboring atoms (e.g. formic acid, Figure 4a), constructing anti-bonding  $\pi$  orbital. In the case of carboxylic acids with functional groups of C=O or C=C neighboring to the C1, i.e.  $\alpha$ -keto acids and unsaturated fatty acids, the resulting  $\pi$  orbitals are extended around these functional groups using 2p atomic orbitals of them. Note that, these  $\pi$  orbitals include a bonding character between C1 and neighboring C atom. This delocalization of the electron would contribute to the stabilization of the LUMO level of the carboxylic acid derivatives.

Compared to the results of catalytic tests, there is a clear tendency that the higher LUMO level of the substrate gives low

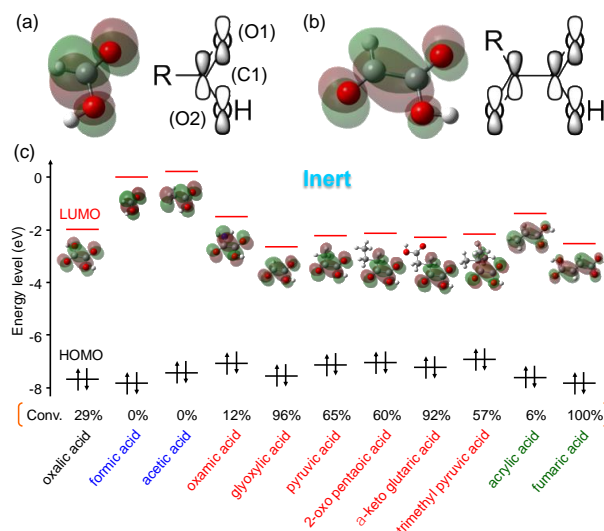


**Figure 4.** (a) A schematic illustration of LUMO of (a) saturated fatty acid (exemplified by formic acid) and (b)  $\alpha$ -keto acid or unsaturated fatty acid (exemplified by glyoxylic acid). (c) A comparison between energy levels of LUMO (and HOMO) and conversions of the substrate in the chronoamperometry. The shape of each LUMO is also illustrated.

reactivity for the hydrogenation reaction (Figure S1), indicating that the hypothesized second step, electron injection, is the most important step in this reaction. Considering this point, we could state that the saturated fatty acid, formic acid and acetic acid, are not easily electrochemically hydrogenated because of the difficulty of electron injection into the substrate due to their high LUMO level (0.002–0.255 eV) derived from the localized anti-bonding  $\pi$  orbital. This also means that the electrons injected from the electrode are usable for hydrogen production that is regarded as a side-reaction in this system. In contrast, almost all of  $\alpha$ -keto acids and unsaturated fatty acids are reactive for this reaction because the electron injection into the substrate successfully proceeds even in the presence of water, i.e. hydrogen evolution is suppressed, due to the stabilized LUMO derived from the extended  $\pi$  orbital. Low reactivity of oxamic acid and acrylic acid clearly indicates that the important factor for the progress of the hydrogenation is not molecular structure of the substrate but the level of LUMO. Note that oxalic acid, which is previously reported as a reactive substrate for the electrochemical hydrogenation reaction, also showed a relatively low LUMO level,  $-1.968$  eV. This is consistent with the tendency described above. Interestingly, the oxalic acid cannot be converted into ethylene glycol (divalent alcohol) but into glycolic acid (monovalent alcohol).<sup>23</sup> Our calculation revealed that the oxalic acid ( $-1.968$  eV) and glyoxylic acid (intermediate for glycolic acid) ( $-2.625$  eV) has the low LUMO level, whereas the glycolic acid has a high LUMO level of  $-0.258$  eV. This means that the glycolic acid is hardly further reduced into the ethylene glycol through the electrochemical hydrogenation due to the high level of LUMO, but can be a final product of the reaction. Based on these considerations, we can assume a border of the energy level of LUMO, determining the reactivity of carboxylic

acid derivatives on anatase TiO<sub>2</sub>, from  $-1.968$  eV (reactive oxalic acid) to  $-1.487$  eV (less reactive oxamic acid). It is interesting that the reactivity of the carboxylic acid derivatives for the electrochemical hydrogenation is predicted simply from LUMO levels.

## 6. DFT studies for composite of a substrate and anatase TiO<sub>2</sub>

To understand better the electro-reduction process on the electrode, we studied selected small substrate molecules interaction with anatase TiO<sub>2</sub> surface using a slab model. The (101) surface is the most commonly observed and recognized as the most stable surface of anatase TiO<sub>2</sub>. It has a zig-zag like structures with alternating lines of fully coordinated six-fold and undercoordinated five-fold Ti atoms. Small molecules generally interact with the five-fold Ti atoms.

Carboxylic acids can be absorbed on the surface in several different geometries, as it was already reported by several other researchers<sup>24-28</sup>. The strongest binding can be observed between deprotonated form of carboxylic acid and a five-fold Ti atom of the surface. Our calculations on acetic acid and oxalic acid result in very similar absorption energies: 118 kJ/mol and 114 kJ/mol for deprotonated, and 67 and 64 kJ/mol for the protonated forms, respectively, which are in good agreement with calculation performed using DFT methods (see references above). As a comparison, we calculated the absorption of alcohols and aldehydes with the same method. Their absorption is much weaker: 15 kJ/mol acetaldehyde and 35 kJ/mol for ethanol, whereas it is 38 kJ/mol for water. This strong absorption of acetic acid to the surface seems to contradict to our experiments showing little absorption on the TiO<sub>2</sub> anode. Some preliminary calculations showed that a solvent effect may be the reason for the difference between the theoretical model and results of experiments. Namely, carboxylic acids with non-polar side chain (e.g acetic acid) form a non-polar surface facing the solution once they absorbed on the oxide surface, instead of the original polar oxide surface. Therefore, water solvent stabilizes much more carboxylic acids with polar side chains (e.g. oxalic acid, glyoxylic acid) when they are absorbed on the surface. Further calculations on this solvent effect will be discussed in a separate manuscript.

These absorption energies are not surprising as they are in line with previous literature data, they give us an important hint about the mechanism of electro-reduction. If reduction from carboxylic to aldehyde occur on the carboxylic group attached to the surface, the difference between absorption energies would add to the reaction energy. This extra  $\sim 100$  kJ/mol makes the anchoring carboxylic group electrochemically inactive. On the other hand, if the electro-reduction occurs on the free carboxylic group of oxalic acid, the difference between absorption energies of reactant and product is small. In conclusion, the strong absorption of the carboxylic group and the significantly weaker aldehyde absorption is the main reason, why simple acids like formic acids or acetic acid cannot be reduced on the electrode.

Our experiments showed that the sidechain of the substrate still can be electrochemically active. In order to explain this reactivity, we studied the interaction between the orbitals of

the electrode and small acids: acetic acid, oxalic acid and glyoxylic acid.

It is useful to picture of the electro-reduction as an electron transfer from the electrode through the anatase TiO<sub>2</sub> conduction bands to LUMOs of the substrate as discussed above. The mutual position of the conduction-band minimum of the composite and the projected density of states (PDOS) of the studied small acids after deprotonation and absorption to the surface is shown in Figure 5. The density of states is dominated by the bands of the anatase TiO<sub>2</sub>, i.e., around the band gap, the valence band mostly consists of p orbitals from O atoms of TiO<sub>2</sub>, and the conduction band is mostly built up from the empty d orbitals of the Ti atoms. The projected density of states (PDOS) of the absorbed substrate are shown in Figures 6b, 6d and 6f. The energy scale is relative to the maximum of valence band, due to inaccuracies of absolute energy scale and for the better

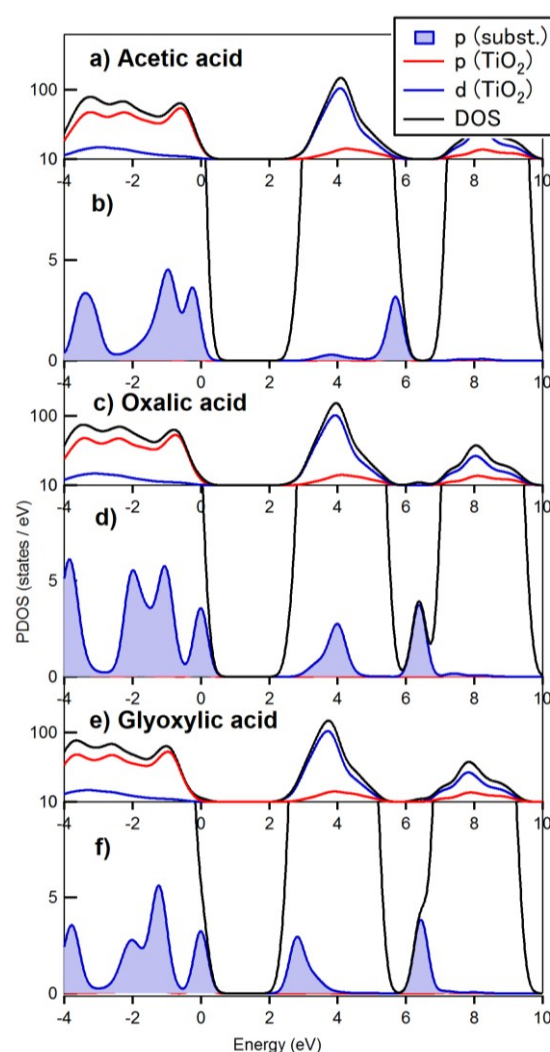


**Figure 5.** The projected density of state (PDOS) of absorbed substrates and TiO<sub>2</sub> compared to the total density of state (DOS): acetic acid (a, b), oxalic acid (c, d) and glyoxylic acid (e, f). All energies are normalized to the valence band maxima. (a, c, e) are scaled to show the total density of states (DOS), whereas b, d and f are zoomed in to show the PDOS of the substrates.

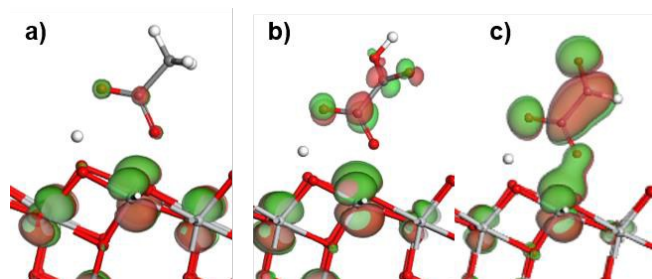


**Figure 6.** Interaction between the substrate orbitals with the conduction band bottom: acetic acid (a), oxalic acid (b) and glyoxylic acid (c).

comparison. After absorption, projected states of acetic acid show a small peak at 4eV and a much more intense at 6eV. These states are the result of the orbital interaction between the substrate LUMO orbitals and the conduction band. Similar states have intensive peaks for both oxalic acid and glyoxylic acid, around 4 and 3 eV (Figures 6d and 6f), respectively, which energies are much better aligned to the conducting band minimum than that of the acetic acid. As we mentioned in the introduction, the alignment of conduction-band-bottom and the LUMO of absorbed substrate is a necessary condition for the electro-reduction, which we can see in the case of oxalic and glyoxylic acid.

The orbital mixing between the substrate LUMO and conduction band (shown in Figure 6) is strikingly different for the three acids. In the case of acetic acid, the orbital is localized on the anchoring carboxylic group, which is electrochemically inert as we discussed above. In the case of oxalic and glyoxylic acid, the empty orbital is delocalized on the substrate and extends to the  $\alpha$ -carbon with the oxo-group, too. This is consistent with the shape of LUMO of the free molecules. The different orbital interactions are also reflected in the amplitudes of the substrate orbitals: while the amplitude of acetic acid orbital is small, those are much bigger in the case of oxalic and glyoxylic acid, showing a strong orbital interaction in the later cases. This strongly supports that electrons from the electrode can directly transferred to the empty orbitals on  $\alpha$ -carbon and electro-reduction is possible.

### 7. Construction of a polymer electrolyte alcohol synthetic cell (PEAEC) for continuous production of an alcoholic compound from a carboxylic acid and water

We suggested possibility of highly selective synthesis of alcoholic compounds from  $\alpha$ -keto acids. For the practical purpose, continuous production of a product seems ideal. In this context, we first developed a flow type electrolyser, namely, a polymer electrolyte alcohol synthetic cell (PEAEC) to produce glycolic acid from oxalic acid. For the construction of PEAEC, we newly prepared a carboxylic acid permeable  $\text{TiO}_2$  cathode and a membrane electrode assembly (MEA).

Efficient diffusion and conversion of substrates are required on the cathode. We thus applied a mesh (Ti-M) or felt type Ti electrode (Ti-F) and directly grew  $\text{TiO}_2$  crystals using Ti species of electrode as a Ti source via hydrothermal method developed by W.-Q. Wu et al.<sup>29</sup> Figures 8a–8c represent scanning electron

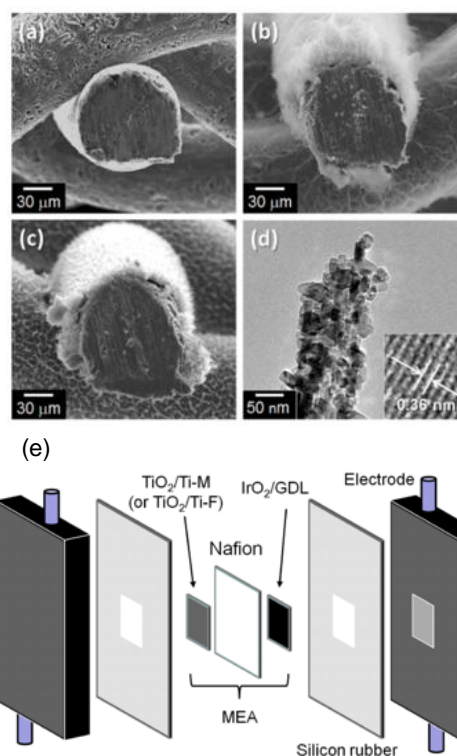


**Figure 7.** Scanning electron microscope (SEM) images of (a) Ti mesh before the hydrothermal reaction, (b) after the first-step reaction taking 12 h ( $\text{H}_2\text{Ti}_2\text{O}_5\text{-H}_2\text{O}$  on Ti mesh), and (c) after the second-step reaction ( $\text{TiO}_2/\text{Ti-M}$ ). (d) A transmission electron microscope (TEM) image of a  $\text{TiO}_2$  fibre deposited on the  $\text{TiO}_2/\text{Ti-M}$  after the two-step hydrothermal reaction (first step: 12 h, second step: 24 h). A magnified fringe pattern is shown in the inset. (e) Assembly of building blocks for the PEAEC.

microscope (SEM) images of Ti mesh before reaction, after the first-step hydrothermal reaction (12 h), and after the second-step reaction. Fibrous solids around Ti lines were formed from Ti species dissolved from metal (Figure 7b). The micro fibres formed on the Ti line were confirmed to be a crystalline  $\text{H}_2\text{Ti}_2\text{O}_5\text{-H}_2\text{O}$ . XRD pattern of the mesh after the second step indicated the formation of anatase  $\text{TiO}_2$  through a hydrolysis of the  $\text{H}_2\text{Ti}_2\text{O}_5\text{-H}_2\text{O}$ . The SEM image of the prepared  $\text{TiO}_2$  on Ti-M ( $\text{TiO}_2/\text{Ti-M}$ ) reveals that a fibrous  $\text{TiO}_2$  directly contacts with Ti electrode (Figure 7c). Figure 7d suggests that the fibre is composed of  $\text{TiO}_2$  grains with diameters of approximately 20–30 nm with good crystallinity, which was recognized from lattice fringes (inset of Figure 7d).

$\text{IrO}_2$  was applied as an anode for water oxidation because of their high catalytic performance and long-term durability in the highly acidic solution such as high-concentration oxalic acid solution. MEA for PEAEC was prepared by pressing  $\text{TiO}_2/\text{Ti-M}$ , Nafion membrane and  $\text{IrO}_2$  at 120 °C. PEAEC was fabricated by attaching the MEA between carbon or Ti electrodes flow channels (Figure 7e). We optimized the PEAEC structure and reaction conditions, and finally achieved almost 100% conversion (99.8%) of 1 M oxalic acid solution, having a

volumetric electric-power capacity of 107 Ah l<sup>-1</sup>, into glycolic acid. Recent optimization of the cell structure and improvement of anode performance by employing lab-prepared nano-structured IrO<sub>2</sub> nanoparticles efficiently enhanced energy conversion efficiency of PEAC.<sup>30</sup> Eventually, fully reconstructed PEAC achieved almost 100% conversion (98.9%) of 3M oxalic acid, which is an almost saturated aqueous solution at operation temperature of the PEAC (60 °C) and has a volumetric electric-power capacity of 321 Ah l<sup>-1</sup>. The energy conversion efficiency<sup>22</sup> was also increased and reached 59.4%. Therefore, PEAC can be regarded as a novel energy storage device to continuously store electric power into a liquid chemical, which is more easily treatable than gaseous and chemically active H<sub>2</sub>.

## 8. Conclusion

We systematically demonstrated electro-reduction of non-aromatic carboxylic acid on anatase TiO<sub>2</sub>, and studied the reaction from both experimental and theoretical point of view. Reactivities of carboxylic acids are experimentally examined using three groups of carboxylic acid derivatives, saturated fatty acid,  $\alpha$ -keto acid, and unsaturated fatty acid. From the adsorption measurements and DFT calculations, the electron injection into the substrate seems to be an important step and that the LUMO level of the substrate is a dominant factor for determination of the reactivity. Under the experimental conditions, the carboxylic group of the selected substrates except for oxalic acid is not reduced on an anatase TiO<sub>2</sub> catalyst, whereas the hydrogenation on the unsaturated groups (C=O or C=C) neighboring to the carboxylic group proceed. We clarify that the saturated fatty acid (formic acid and acetic acid) is not reactive and that some of the substrates (oxamic acid and acrylic acid) is much less reactive than the others. Calculations also showed that the anchoring carboxylic group of the substrates is electrochemically inactive due to their strong binding to the electrode surface.

From these findings, we can develop crucial factors for promotion of electro-reduction of carboxylic acids as following.

(1) Semiconductor catalyst having a HOMO level located at sufficiently higher than the LUMO of a carboxylic acid

(2) Extension of the conjugation system around the carboxyl group of the substrate to stabilize transition states

(3) Highly developed hybridization between LUMO of a substrate molecule and orbitals of catalyst surface that enhance charge transfer from electrode to substrate

Thus, present perspective paper unravels the hidden mechanism for the electro-reduction of carboxylic acids on TiO<sub>2</sub> surface, which is not easily achievable. Further efforts based on our findings would achieve highly active electro-catalysts which are available for more versatile electrocatalytic reactions. We first constructed a flow-type electrolyser built from highly selective anatase TiO<sub>2</sub> catalyst for the continuous production of an alcoholic compound from environmentally friendly carboxylic acid, which enables direct and highly efficient electric power storage. All the efforts shown here will contribute to establishing a society that can develop sustainably with reduced environmental loads.

This work is partly supported by Core Research for Evolutional Science and Technology (CREST), Japan Science and Technology Agency (JST).

## Conflicts of interest

There are no conflicts to declare.

## Acknowledgements

This work was supported by the International Institute for Carbon Neutral Energy Re-search (WPI-I<sup>2</sup>CNER), sponsored by the World Premier International Research Center Initiative (WPI). This work was supported by MEXT KAKENHI Grant Number JP12852953 and JP18H05517, and JST-CREST, Japan.

## Notes and references

1. A. Dutta, C. E. Morstein, M. Rahaman, A. Cedeño López and P. Broekmann, *ACS Catal.*, 2018.
2. X. Bai, W. Chen, C. Zhao, S. Li, Y. Song, R. Ge, W. Wei and Y. Sun, *Angew. Chem.*, 2017, 56, 12219-12223.
3. N. Han, Y. Wang, H. Yang, J. Deng, J. Wu, Y. Li and Y. Li, *Nat. commun.*, 2018, 9, 1320
4. S. Ma, M. Sadakiyo, R. Luo, M. Heima, M. Yamauchi and P. J. Kenis, *J. Power Sources*, 2016, 301, 219-228
5. S. Ma, M. Sadakiyo, M. Heima, R. Luo, R. T. Haasch, J. I. Gold, M. Yamauchi and P. J. Kenis, *J. Amer. Chem. Soc.* 2016, 139, 47-50.
6. Y. Zhou, F. Che, M. Liu, C. Zou, Z. Liang, P. De Luna, H. Yuan, J. Li, Z. Wang and H. Xie, *Nat. Chem.*, 2018, 1
7. C.-T. Dinh, T. Burdyny, M. G. Kibria, A. Seifitokaldani, C. M. Gabardo, F. P. G. de Arquer, A. Kiani, J. P. Edwards, P. De Luna and O. S. Bushuyev, *Science*, 2018, 360, 783-787.
8. J. Edwards, *Catal. Today*, 1995, 23, 59-66.
9. 9.Y. Lin and S. Tanaka, *Appl. Microbiol. Biot.*, 2006, 69, 627-642.
10. Y. Muranaka, A. Iwai, I. Hasegawa and K. Mae, *Chem. Eng. J.*, 2013, 234, 189-194
11. J. Pritchard, G. A. Filonenko, R. van Putten, E. J. Hensen and E. A. Pidko, *Chem. Soc. Rev.*, 2015, 44, 3808-3833.
12. T. J. Korstanje, J. I. van der Vlugt, C. J. Elsevier and B. de Bruin, *Science*, 2015, 350, 298-302.
13. G. H. Coleman, H. L. Johnson, *Org. Synth.*, 1955, Coll. Vol. III, 60.
14. C. Mettler, *Chem. Ber.*, 1916, 39, 2933.
15. F. Zhao, F. Yan, Y. Qian, Y. Xu, C. Ma, *J. Electroanal. Chem.*, 2013, 698, 31-38.
16. D. J. Pickett, K. S. Yap, *J. Appl. Electrochem.*, 1974, 4, 17-23.
17. F. Goodridge, L. Lister, R. E. Primley, *J. Appl. Electrochem.*, 1980, 10, 55-60.
18. R. Watanabe, M. Yamauchi, M. Sadakiyo, R. Abe and T. Takeguchi, *Energ. Environ. Sci.*, 2015, 8, 1456-1462.
19. M. Yamauchi, N. Ozawa and M. Kubo, *The Chem. Rec.*, 2016, 16, 2249-2259.
20. T. Fukushima, S. Kitano, S. Hata and M. Yamauchi, *Sci. Tech. Adv. Mater.*, 2018, 19, 142-152.
21. S. Kitano, M. Yamauchi, S. Hata, R. Watanabe and M. Sadakiyo, *Green Chem.*, 2016, 18, 3700-3706.
22. M. Sadakiyo, S. Hata, X. Cui and M. Yamauchi, *Sci. Rep.*, 2017, 7, 17032.



## COMMUNICATION

Journal Name

23. W. Rachmady, M. A. Vannice, *Journal of Catalysis*, 2000, 192, 322-334.
24. C. Spreafico, F. Schiffmann, J. VandeVondele, *J. Phys. Chem. C* 2014, 118, 6251-6260.
25. C. Anselmi, E. Mosconi, M. Pastore, E. Ronca, F. de Angelis, *Phys. Chem. Chem. Phys.* 2012, 14, 15963-15974.
26. A. Vittadini, A. Selloni, F.P. Rotzinger, M. Gratzel, *J. Phys. Chem. B* 2000, 104, 1300-1306.
27. M. Chan, T. Carrington, S. Manzhos, *Phys. Chem. Chem. Phys.* 2013, 15, 10028-10034
28. S. Manzhos, G. Giorgi, and K. Yamashita, *Molecules* 2015, 20, 3371-3388.
29. W.-Q. Wu, H.-S. Rao, Y.-F. Xu, Y.F. Wang, C.-Y. Su, D.-B. Kuang, *Sci. Rep.* 2013, 3, 1892.
30. T. Fukushima, M. Higashi, S. Kitano, T. Sugiyama, M. Yamauchi (submitted to *Catal. Today*)